MUSIC algorithm for vibro-acoustic defect detection

Philip Becht[1,2*], Elke Deckers[1,2], Claus Claeys[1,2], Bert Pluymers[1,2], Wim Desmet[1,2]

[1] KU Leuven,
Dept. of Mechanical Engineering, Celestijnenlaan 300, box 2420, 3001, Leuven, BELGIUM
Email: Philip.Becht@kuleuven.be

[2] member of Flanders Make

ABSTRACT

Defect detection based on the processing of ultrasonic signals using the MUSIC algorithm is a recent subject of research. This paper suggests to make use of the sub-wavelength detection accuracy that can be achieved with the MUSIC algorithm to lower the testing frequency. This allows the application of the detection strategy to periodic and heterogeneous materials, such as honeycomb structures, where defect detection at higher frequencies becomes difficult, due to the complex scattering behavior. Furthermore the sound radiated from the structure in the surrounding air can be picked up with microphones to replace structural sensors, with the consequence that coupling problems between structure and sensors, e.g. due to badly glued sensors, are avoided automatically and the time for setting up the measurement is reduced. In this paper, it is demonstrated using the example of an A3 Aluminum plate radiating in a half space that the detection accuracy of a vibro-acoustic test-setup (excitation: structural, sensor: microphone) is equal to that of a purely structural measurement (excitation: structural, sensor: structural).

1 INTRODUCTION

A commonly used method in the field of ultrasonic nondestructive testing (NDT) is defect detection based on ultrasonic waves. More recently, the combination of ultrasonic waves with the concept of time-reversal (TR) was introduced to NDT [1]. One sub-group of TR methods is the so called TR-MUSIC algorithm, where MUSIC stands for MUltiple SIgnal Classification. This technique proved to be very robust to measurement noise and reaches an imaging resolution that is significantly smaller than the wavelength [2, 3].

The latter feature allows to lower the testing frequency, while still being able to generate an accurate image of the defect location. This comes with the downside of a reduced interaction between incident wave and defect. On the other hand, e.g. in case of periodic structures characterized by the repetition of a unit cell (UC), ultrasonic waves can significantly scattered at the boundaries of the UC and therefore in these cases be problematic for defect detection of the entire structure. At lower frequencies, and thus larger wavelength, the scattering at the boundaries of the UC decreases, which is why waves in this frequency range, then can be employed to globally monitor the health status.

Furthermore, lowering the frequency enables to measure the radiation of structural vibrations in the surrounding air, which would not be possible at higher frequencies due to the stronger damping for a given distance of propagation. The advantage of employing microphones instead of structural sensors are versatile. E.g., one consequence is that no sensors need to be attached to the structure, which automatically avoids problems with the coupling. Furthermore, it avoids wave scattering at the sensors and saves time.

This paper provides a numerical study with the focus to determine the ability to use the radiation of structural vibrations in the surrounding air for the detection of a small defect (small as compared to the wavelength).

2 MUSIC IMAGING

The MUSIC algorithm is based on the idea to decompose the so called multi-static data matrix $\boldsymbol{K}$ in components belonging to a signal space and components belonging to a noise space. In a mechanical system the elements of $\boldsymbol{K}$ at one discrete frequency are

$$k_{m,n} = k_{D,m,n} - k_{I,m,n}, \tag{1}$$

with $k_{\cdot,m,n}$ the transfer function from the n-th point of excitation to the m-th measurement point in the defected (subscript *D*) and the intact (subscript *I*) structure, respectively. The transfer path can be purely structural or vibro-acoustic.

The decomposition of $\boldsymbol{K}$ is done by means of a singular value decomposition

$$\boldsymbol{K} = \boldsymbol{G}_E \boldsymbol{V} \boldsymbol{G}_S^H, \tag{2}$$

where $\boldsymbol{G}_E = \left[\boldsymbol{g}_{E,1}, \boldsymbol{g}_{E,2}, \dots, \boldsymbol{g}_{E,N}\right]$ and $\boldsymbol{G}_S = \left[\boldsymbol{g}_{S,1}, \boldsymbol{g}_{S,2}, \dots, \boldsymbol{g}_{S,M}\right]$ are matrices containing the left and right hand side singular vectors, $\boldsymbol{V}$ is the matrix of the singular values and the superscript *H* denotes the complex conjugate transpose. $\boldsymbol{G}_E$ and $\boldsymbol{G}_S$ are $N \times N$ and $M \times M$ matrices, where *N* is the number of excitation points and *M* is the number of sensors. Throughout the paper quantities referring to the excitation are indicated with subscript *E*, those referring to sensors with subscript *S*.

$\boldsymbol{V}$ contains *P* singular values corresponding to the signal space and $\min(M, N) - P$ singular values corresponding to the noise space. According to this definition $\boldsymbol{G}_E$ can be split in a part corresponding to the signal space with singular vectors $\boldsymbol{g}_{E,i \leq P}$ and a part corresponding to the noise space with singular vectors $\boldsymbol{g}_{E,i>P}$. The choice of *P* is done as suggested in [4].

For the case of point scatterers under the Born approximation, *P* is equal to the number of scatterers. Following He and Yuan [3], for this case, due to the orthogonality of the singular values, the scalar product between $\boldsymbol{g}_{E,i\leq P}$ and a vector containing the transfer functions from the points of excitation to an arbitrary point *x* in the intact structure, $\boldsymbol{k}_{I,E}(x)$ is 0 only if *x* is not equal to the location of the defect x_i. Making use of the orthogonality between signal and noise space, this property can be used to calculate an image function, which peaks at all locations $x = x_i$

$$I(x) = \frac{1}{\sum_{i=P+1}^{\min\{M,N\}} \left\langle \boldsymbol{g}_{E,i}, \boldsymbol{k}_{I,E}(x) \right\rangle}. \tag{3}$$

The theory can also be extended to scatterers with finite extent, with the outcome that $I(x)$ reaches its maximum at the location of the scatterers. The principle of imaging remains unchanged.

3 NUMERICAL ANLAYSIS

In this section the above described theory is applied to a simply supported A3 Aluminum plate ($E = 7 \cdot 10^{10}$ N/m^2, $\rho = 2700$ kg/m^3, $\nu = 0.3$, structural damping coefficient = $5 \cdot 10^{-4}$) of 2mm thickness radiating in a half space filled with air. A square damage of 3mm x 3mm is assumed, which is modelled by removing one element. The plate is excited at 8000Hz, which results in a wavelength of 49mm. The mesh is composed of linear 2D elements with an edge length of 3mm.

3.1 Imaging based on structural vibration

At first the location of the defect is searched based on Equation (3) with randomly chosen 27 structural excitation points. The out-of-plane displacement of the plate is calculated at 27 arbitrarily chosen locations, which serve as virtual sensors. *P* is chosen as 9, following [4].

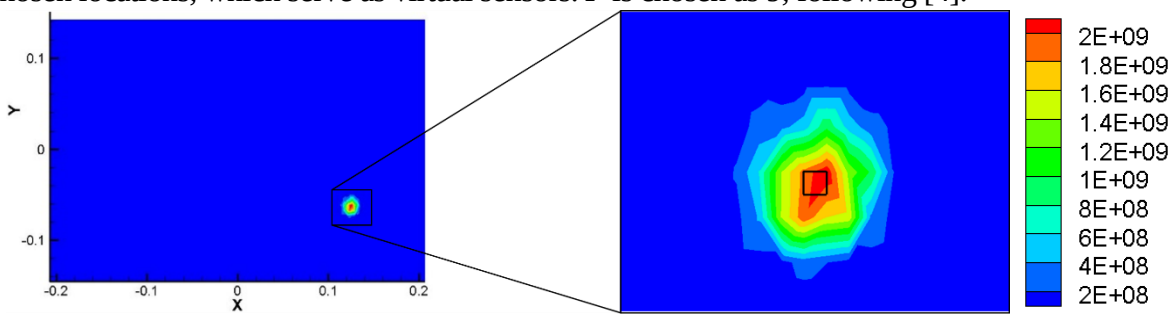

Figure 1. Purely structural imaging result ($I(x)$) of Equation 3 for the entire plate (left) and zoom to the defected region (right). Deleted element is indicated with black square in the right figure.

As can be seen from Figure 1, the maximum of the image index is shown at the top right corner of the defect. Furthermore it is evident that the region of the defect and its direct vicinity is clearly separated form the undefected regions of the plate. Assuming a possible defect in the region around the maximum, until the amplitude is lowered by a factor 10, gives a circle of roughly 20mm diameter, which proves that defects can be located with a sub-half-wavelength accuracy.

3.2 Imaging based on vibro-acoustic measurement

In this section the imaging is done based on the same equation with the same 27 structural excitation points already used in the previous section. As opposed to section 3.1, now only microphone measurements (pressure) are used for the imaging. The 27 (equal to the number of structural sensors in 3.1) microphones are located at randomly chosen points on a half-sphere with 620mm diameter and the center coinciding with the center of the plate. Also in this case *P* is chosen equal to 9.

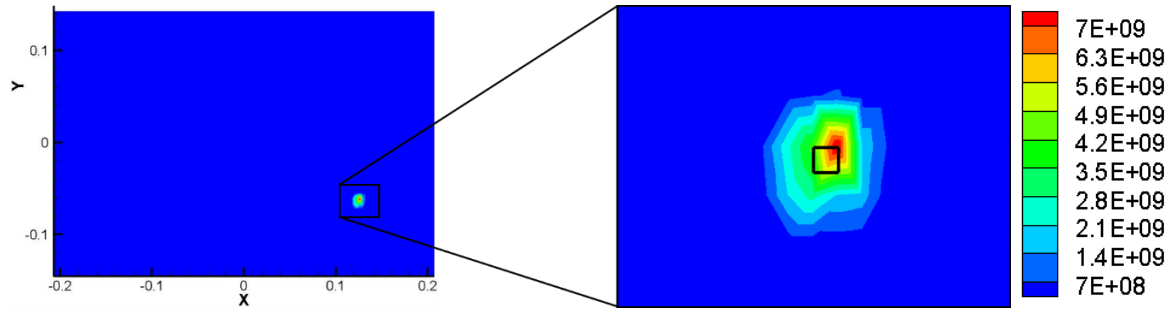

Figure 2. Vibro-acoustic imaging result ($I(x)$) of Equation 3 for the entire plate (left) and zoom to the defected region (right). Deleted element is indicated with black square in the right Figure.

As in Figure 1, also in the case of vibro-acoustic imaging (Figure 2), the maximum of the image index is located at the top right corner of the defect. Although the maximum in Figure 2 is more extreme than that in Figure 1, the area of a possible defect in the vibro-acoustic case is even smaller than it is in the purely structural case.

Further numerical simulations illustrate that the number of measurement and excitation points in both cases can be reduced to P+1 without a significant loss of detection accuracy. Also the stability of the algorithm at the presence of random measurement errors, which is reported in literature, can be observed, as will be shown at the conference presentation.

4 CONCLUDING REMARKS

As a numerical example, it is shown that the MUSIC algorithm can be used for the detection of a defect in a structure, while only microphone measurements are used. The comparison between a purely structural and a vibro-acoustic case suggests that the detection accuracy due to the vibro-acoustic measurement does not decrease. In both cases the location of a defect can be narrowed down to an area significantly smaller than the structural wavelength at the excitation frequency.

ACKNOWLEDGEMENTS

The European Commission is gratefully acknowledged for their support of the ANTARES project (GA606817). Furthermore, the authors acknowledges the financial support from Strategic Initiative Materials in Flanders (SIM) through the MADUROS,DEMOPROCI-NDT Program. The research of E. Deckers is funded by a grant from the Fund for Scientific Research – Flanders (F.W.O.). Also the Research Fund KU Leuven is gratefully acknowledged for its support.

REFERENCES

[1] H. Sohn, H. Park, W. Hyun, K. Law and C. Farrar. Damage detection in composite plates by using an enhanced time reversal method. *Journal of Aerospace Engineering*. 20(3):141-151, 2007.

[2] H. Choi, Y. Ogawa, T. Nishimura and T. Ohgane. Time-reversal MUSIC imaging with time-domain gating technique. *IEICE transactions on communications*. 95(7):2377-2385, 2012.

[3] J. He and F.-G. Yuan. Lamb wave-based subwavelength damage imaging using the DORT-MUSIC technique in metallic plates. Structural Health Monitoring. 15(1):65-80, 2016.

[4] E. Marengo, F. Gruber and F. Simonetti. Time-reversal MUSIC imaging of extended targets. IEEE Transactions on image processing. 16(8):1967-1984, 2007.